Solar Energy Vol. 35, No. 4, pp. 311–320, 1985
Printed in the U.S.A.

0038-092X/85 $3.00 + .00

SOLAR TRANSMITTANCE CHARACTERISTICS OF EVACUATED TUBULAR COLLECTORS WITH DIFFUSE BACK REFLECTORS

P.-H. THEUNISSEN† and W. A. BECKMAN
Solar Energy Laboratory, University of Wisconsin-Madison, 1500 Johnson Drive, Madison, WI 53706, U.S.A.

(*Received* 27 *September* 1983; *revision received* 11 *February* 1985; *accepted* 12 *February* 1985)

Abstract—The partition matrix between light sources and light sinks is introduced to evaluate the transmittance properties of optically asymmetric collectors constructed with evacuated tubes. A ray tracing model is used to compute its elements. Curve fits to the ray tracing results are provided. The effects of polarization are discussed. Comparisons with previously published results are presented in order to check the accuracy of the proposed model. The beam and diffuse transmittance of a tubular cover are calculated and their dependency on the tube orientation investigated. The biaxial incidence angle modifier product is extended to evacuated tube collector arrays with a diffuse back reflector, providing a simple interpolation process for the beam transmittance. An effective beam direction for diffuse radiation is computed so that transmittances for ground reflected radiation and sky diffuse radiation can be calculated from biaxial incidence angle modifier measurements.

1. INTRODUCTION

Collector efficiency is a strong function of the collector overall heat loss coefficient. An evacuated glass tube provides outstanding thermal insulation by suppressing internal conduction and convection losses. This geometry has been considered for several years by a number of companies[1].

The anisotropic nature of these collectors yields angularly dependent optical efficiencies. Consequently, the transmittance of beam radiation will be a function of two angles θ and ψ, as shown in Fig. 1. The angle θ is the classical flat-plate collector incidence angle and the angle ψ is the azimuth angle formed in the collector plane between the longitudinal plane and the plane given by the collector normal and the beam radiation.

Experimental measurements of the angular dependence of beam radiation transmittance for tubular covers are rare. Herrick[2] found that the normal beam transmittances reported in the literature for tubular covers vary between 0.78 and 0.90 and that little information is available about the relationship between beam transmittance and incidence angle. Herrick presents experimental results for beam transmittance for both the transversal and longitudinal planes. His measurements are in good agreement with experimental results of Jones[3] for incidence angles less than 30°. No data were found in the literature for the sky and ground diffuse transmittance.

This study of evacuated tube collector (ETC) arrays will be limited to those with a diffuse back reflector. The optical properties of collectors with specular back reflectors (i.e. nonimaging concentrating collectors) has been the subject of studies by McIntire and Reed[4], Window and Basett[5] and others. The ETC family can be split in two classes of absorber geometry: collectors with cylindrical absorbers (Owens-Illinois, General Electric[4]) and collectors with flat absorbers (Philips[6], Sanyo[7], Philco[8]). Using a Monte Carlo ray tracing technique, Window and Zybert[9] present normal beam transmittance and diffuse transmittance results for ETC arrays having a few different cylindrical absorber configurations. A simple tool was provided to predict the optical efficiencies of those collector arrays.

The present study extends previous work by developing correlations of ray tracing results to compute the beam, sky and ground diffuse transmittance for a wide range of ETC designs and tubular cover designs. In addition, an algorithm is provided to interpolate between the transversal and longi-

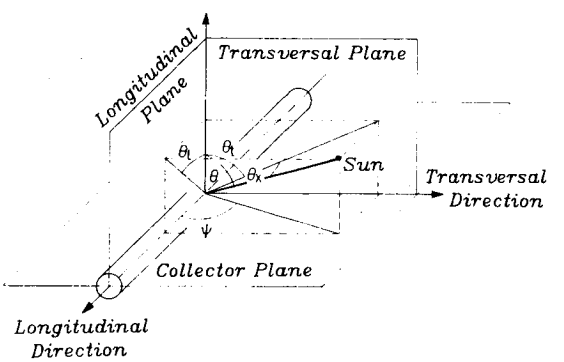

Fig. 1. Coordinate system of the evacuated tube collector array.

† Current address: von Karman Institute for Fluid Dynamics, 72 Chausses de Waterloo, 1640 Rhode St., Genese, Belgium

tudinal incidence angle modifiers defined by the ASHRAE 93-77 test procedure [10]. Finally, as was done for flat-plate collectors[11], the transmittance for diffuse ground reflected or diffuse sky radiation is expressed as an equivalent incidence direction for beam radiation. With this correlation, it is possible to compute the diffuse transmittance of a given collector from its transversal and longitudinal beam transmittance curves.

II. GEOMETRY OF THE EVACUATED TUBE COLLECTOR ARRAY AND TUBULALR COVER

The ETC array under consideration is composed of equally spaced individual tubes lying parallel to a diffuse reflector plane. It is assumed that the array is infinite in both longitudinal and transversal directions to eliminate edge effects. The geometry of an ETC array is defined by the absorber shape (flat or cylindrical) and three sizing parameters as shown in Fig. 2: W, width or diameter of the absorber; C, spacing between the tubes; and D, distance between the back reflector and the center line of the glass tubes. These lengths are expressed with the glass tube outside diameter as reference.

The tubular cover flat-plate collector is a limiting case of the ETC design. It is characterized by $C = 1$ (i.e. no spacing between the tubes), $W = 0$ (i.e. no absorber inside the tubes) and with the diffuse back reflector as the collector absorber.

III. COMPUTATION PROCEDURE

In either the ETC systems or the tubular cover system, three different light sources will have to be considered: beam radiation, characterized by the angles θ and ψ; diffuse sky radiation, characterized by the collector slope β, which fixes the view factor between the collector and the sky dome; and the diffuse ground reflected radiation, also characterized by the angle β.

Energy from each of these light sources, in passing through the system of Fig. 2, will be distributed according to optical laws to four light sinks: the absorber surface of the collector array, initially assumed to absorb all incident radiation; the glass envelope which will absorb radiation if its optical extinction coefficient is nonzero; the surroundings which absorb all radiation reflected back to either the ground or the sky; and the diffuse back reflector, initially assumed to absorb all incident radiation. Reflection from this back surface will be accounted for by assuming it to be a fictitious diffuse light source.

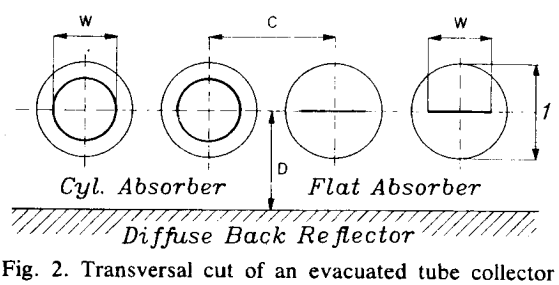

Fig. 2. Transversal cut of an evacuated tube collector array.

The light partition matrix, R, between the light sources and sinks has 16 elements.‡ Each element, R_{ij}, represents the fraction of energy coming from the source i that is absorbed by sink j; the index i and j are defined by

i, *light source*	j, *light sink*
1 beam	1 absorber
2 sky diffuse	2 glass cover
3 ground diffuse	3 surroundings
4 back reflector	4 back reflector

The R_{1j} elements are functions of the incoming beam angles θ and ψ, while the elements R_{2j} and R_{3j} are functions of the slope of the collector. The elements R_{4j} are independent of collector orientation. From conservation of energy, each row of the partition matrix has to satisfy the relation:

$$\sum_{j=1}^{4} R_{ij} = 1, \text{ for all } i. \tag{1}$$

Eberlein [13] showed that if the back reflector is far enough from the center line of the tubes to satisfy the following relations

$$\text{if } C < 2 \text{ and } D > 1.5$$

or

$$C > 2 \text{ and } D/C > 0.75, \tag{2}$$

then D does not have a significant influence on the optical efficiency. This means that the incident light falling on the back reflector may be assumed to be uniformly distributed. Equivalent conclusions are also reported by Window and Zybert[9]. These inequalities are assumed to hold in all subsequent discussion.

The fraction of the energy transmitted to the absorber from source i, τ_i, can then be expressed as

$$\tau_i = R_{i1} + R_{i4}\rho_4\tau_4, \tag{3}$$

where ρ_4 is the diffuse reflectance of the uniformly illuminated back reflector. The first term is the radiation from source i that does not reach the back reflector but is intercepted by the absorber; the second term is the radiation from source i that reflects off the back reflector and is then transmitted to the absorber. τ_4, the transmittance to the ab-

‡ The elements of the partition matrix are similar to the absorption factors defined by Gebhart[12] for solving gray, diffuse thermal radiation problems. However, the partition matrix formulation does allow for specular reflection and nondiffuse radiation sources.

sorber when the back reflector is considered to be a source, can be expressed as

$$\tau_4 = R_{41} + R_{44}\rho_4\tau_4, \quad (4)$$

where, in a manner similar to eqn (3), the first term represents the transmission to the absorber from the diffuse source back reflector and the second term represents the energy leaving the back reflector that returns to the back reflector, is reflected, and ultimately transmitted to the absorber. Eliminating τ_4 from eqns (3) and (4) yields

$$\tau_i = R_{i1} + R_{i4}\rho_4 R_{41}/(1 - R_{44}\rho_4) \quad (i = 1, 2, 3). \quad (5)$$

This transmittance, when multiplied by the absorber surface solar absorptance, α_1, approximates the fraction of the energy from source i that is absorbed by the absorber. In the solar energy literature this is referred to as the transmittance–absorptance product and given the symbol $(\tau\alpha)$. This transmittance–absorptance product does not include secondary effects resulting from imperfect absorption by the absorber. The absorber may have an angular dependence of solar absorptance whereas the absorptance has been assumed to be independent of direction. Also, radiation reflected from the absorber is assumed not to return to the absorber. These assumptions will be discussed later in more detail.

The tubular cover is a limiting case of eqn (5) and will be discussed in detail in the next section. For a flat-plate collector with a tubular cover, the back reflector is the absorber and the transmittance of the cover is

$$\tau_i = R_{i4} \quad (i = 1, 2, 3). \quad (6)$$

The three transmittances given by eqns (5) and (6) require values from the partition matrix R. Advantage is taken of the symmetry of the array by considering only one region as shown in Fig. 3, composed of one evacuated tube above the back reflector located between two mirrorlike vertical walls spaced $C/2$ from the center. Although this region is also geometrically symmetrical about the longitudinal plane through the tube center, it cannot be further reduced since this plane is not a symmetry plane for the beam radiation.

Since a plane parallel to the back reflector and passing through the center line of the glass tubes defines a plane of symmetry, the partition of light reflected by a back reflector that satisfies eqn (2) is identical to the partition of light from the diffuse sky source for a horizontal collector. Thus for $\beta = 0$, the following relations exist between R_{2j} and R_{4j}

$$R_{41} = R_{21} \quad R_{42} = R_{22} \quad (7)$$
$$R_{43} = R_{24} \quad R_{44} = R_{23}.$$

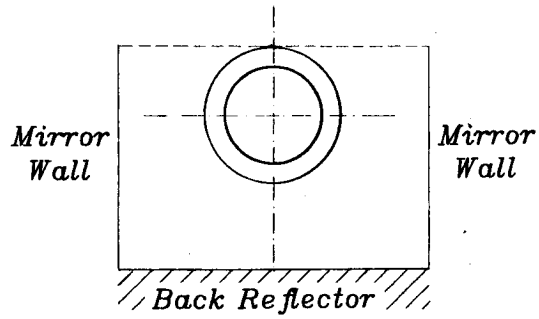

Fig. 3. Section of a symmetry cell analyzed by the ray tracing algorithm.

Ray tracing is used to find numerical values of the partition matrix. The radiation entering the cell is divided into bins of constant width. For the beam radiation at a particular angle no further division is necessary, but for diffuse radiation it is necessary to also consider a number of constant solid angle bins to take into account the isotropic feature of the diffuse radiation. Parametric studies revealed that 50 bins, uniformly distributed across the aperture are required to accurately determine the transmittance at a particular angle. One hundred different solid angle bins at each aperture bin were required to accurately determine the sky and ground diffuse transmittances. Each bin is handled by considering its center ray and following it until it reaches one of the four light sinks.

Several assumptions are made in order to reduce the complexity of computation. The wall thickness of the glass tube is assumed to be negligible compared to its diameter with the consequence that rays do not bend when passing through the glass. This assumption permits the use of classical expressions for glass cover transmittance, reflectance and absorptance, for example, as given in reference[14]. The light is assumed to remain unpolarized in spite of the different optical properties for the parallel and perpendicular components of reflections. This approximation will be analyzed more carefully in the tubular cover study. Finally, as already indicated, the absorptance of the collector absorber is assumed to be perfect. The transmittance–absorptance product will be computed using the transmittance figure resulting from the ray tracing algorithm and the normal incidence value of the absorptance. Window and Zybert [9] report a slight underprediction of $(\tau\alpha)$ as a consequence of this approach for both the incident beam and the diffuse radiation. For off-normal beam radiation it will be shown that the transmittance has a stronger angular dependence than the absorptance which remains essentially constant until an incidence angle of 60°.

Unless otherwise specified, the following ray tracing results were obtained using the properties of a "water white" glass having an index of refraction of 1.526 and an extinction coefficient of 0.

The tubular cover optical properties were obtained with $C = 1$, $W = 0$ and $\rho_4 = 0$. The ETC array was investigated for both flat and cylindrical absorber over the following range of parameters: $0.3 < W/C < 1$; $0.6 < W < 1$; $0.0 < \rho_4 < 1$.

IV. TUBULAR COVER

The tubular cover was selected to investigate the implications of the unpolarized light assumption since all the incoming radiation crosses at least two glass layers and a significant fraction of the incoming radiation undergoes multiple reflections inside and between the glass tubes. For beam radiation in the transversal plane, the parallel and perpendicular components of the light proceed through successive transmissions and reflections without any change in direction and, thus, with an increasing degree of polarization. For the other beam directions, the two components of the light will be transmitted and reflected with perpendicular and parallel directions different at each interface. These successive interactions will redistribute the radiation between perpendicular and parallel directions, and help maintain the unpolarized character.

Transversal beam transmittances for the perpendicular and parallel components are computed with the ray tracing algorithm using the perpendicular and parallel glass cover transmittance and reflectance expressions given in references [14] and [15]. Results are presented in Table 1 versus the incidence angle θ along with the resulting average transmittance defined by:

$$\bar{\tau} = (\tau_{\parallel} + \tau_{\perp})/2 \qquad (8)$$

Also presented is τ_1, the beam transmittance of the tubular cover computed with the unpolarized assumption.

Although the $\tau_{\parallel}$ and $\tau_{\perp}$ components of the transmittance are quite different, the average transmittance, $\bar{\tau}$, is very nearly equal to the unpolarized transmittance, τ_1. Actually, significant polarization occurs only around the Brewster angle[15], which represents only a small portion of the incidence angles in which beam radiation from a given direction hits the glass tube. The good agreement between $\bar{\tau}$ and τ_1 justifies the unpolarized light assumption.

Ray tracing results for the beam transmittance are presented in Fig. 4 versus the incidence angle

Table 1. Effect of polarization on the transmittance computation

Incidence angle ψ	$\tau_{\parallel}$	$\tau_{\perp}$	$\bar{\tau}$	τ_1
0	0.826	0.941	0.870	0.874
20.	0.821	0.911	0.866	0.867
40.	0.794	0.899	0.846	0.845
60.	0.696	0.860	0.778	0.776
80.	0.445	0.693	0.569	0.554

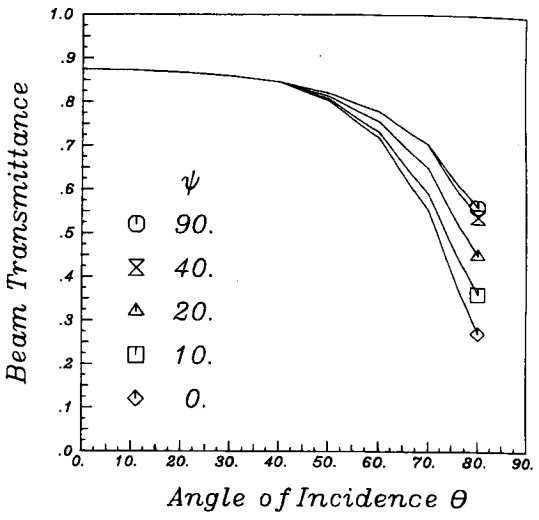

Fig. 4. Beam transmittance of a tubular cover.

θ and the azimuth angle ψ. The normal transmittance is found to equal 0.874. This figure is in good agreement with the experimental results $\tau = 0.87$ of Jones[3] and $\tau = 0.885$ of Herrick[2]. However, the ray tracing results do not reproduce the maximum transmittance of 1.0 at $\theta = 70°$ claimed by Herrick for the transversal transmittance. A discussion of Herrick's experimental results is reported in reference [16].

An F-Chart 4.1[17] analysis shows that the shape of the transmittance curve at incidence angles greater than 60° does not significantly affect the solar energy delivery of a system using south facing collectors with the slope equal to the latitude. The low solar radiation level associated with high incidence angles is the reason for this conclusion. Hence, the range of interest for the incidence angle is between 0° and 60°. Within this domain, Fig. 4 shows that the beam transmittance of a tubular cover is nearly independent of the azimuth angle, and thus insensitive to the tube orientation. The beam transmittance can be considered as a single curve and presented in the ASHRAE 93-77 convention (see [14], p. 263) with a mean incidence angle modifier coefficient, b_o, of -0.15 and a normal incidence value of 0.874.

In the following discussion of diffuse transmittance it is assumed that the line of intersection of the collector plane with the ground is parallel to the transversal plane. For a south facing collector this means that the tube axes are in the north–south plane. This restriction does not have a significant impact on the sky diffuse transmittance since the beam transmittance, which must be integrated over the sky dome to obtain the diffuse transmittance, is almost independent of the tube orientation.

The diffuse transmittances obtained with the ray tracing model are presented in Fig. 5 as a function of the collector slope. The sky diffuse transmittance is 0.794 for a horizontal surface and remains nearly

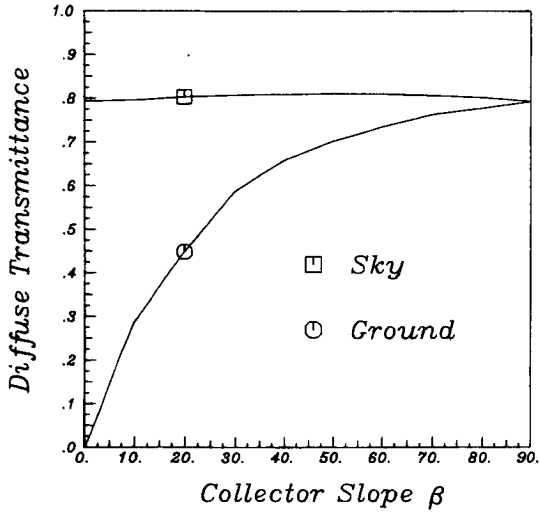

Fig. 5. Diffuse transmittance of a tubular cover.

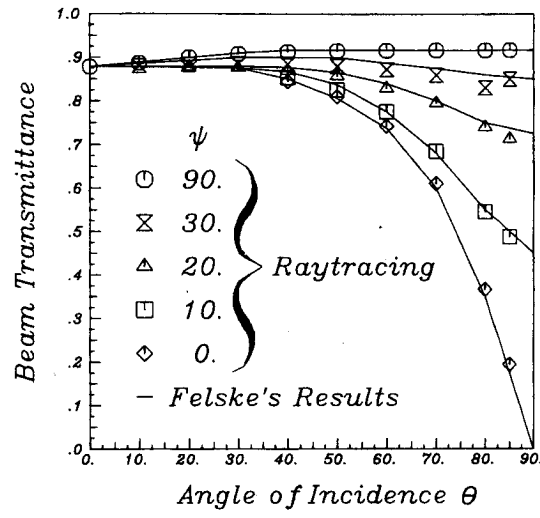

Fig. 6. Beam transmittance of a flat absorber–evacuated tube collector without multiple reflection ($W = 1$).

constant to 90°, with a slight maximum near $\beta = 45°$. This same trend was reported by Brandemuehl and Beckman[11] for flat-plate collectors. The ground diffuse transmittance is close to the sky diffuse transmittance for slopes greater than 40° (0.82 for τ_2 and 0.65 for τ_3 at 40°). Below 40° the difference increases sharply but at these large angles the product of the ground-to-collector view factor and the ground reflectance is less than 3%, and negligible errors occur by assuming that the ground diffuse transmittance is equal to the sky diffuse transmittance.

V. EVACUATED TUBE COLLECTOR ARRAY

V.1 *Comparison with previous results*

Felske[18] presents $\tau_i'(\theta, \psi)$, the beam transmittance of a single tube calculated by neglecting all multiple reflections, for a flat absorber with $W = 1$. Felske's results are in good agreement with the ray tracing calculations as shown in Fig. 6. Due to the cylindrical shape of the cover tube, the transversal transmittance, $\tau_i'(\theta, \psi = 90°)$, increases slightly with the incidence angle. This is so, since for $\theta = 0°$, some part of the beam radiation experiences every incidence angle from 0° to 90° whereas at $\theta = 45°$ for example, the incidence angle varies only between 0° and 45°. The longitudinal transmittance $\tau_i'(\theta, \psi = 0°)$, decreases with θ since the mean incidence angle on the glass cover increases with θ.

Window and Zybert[9] present normal beam and sky diffuse transmittances for a cylindrical absorber ETC array as a function of the spacing C between the tubes. Figure 7 illustrates the good agreement between their results and those obtained with the present ray tracing model, using a glass extinction coefficient of 5 m^{-1} and a glass thickness of 2 mm. These curves show a strong dependency of the optical efficiencies on the tube spacing.

The ray tracing algorithm was also checked with the results of the Owens-Illinois "Sunpack Model 1004 Series Collector"[19] water-filled, cylindrical absorber ETC. The experimental transmittances shown in Fig. 8 were computed from incidence angle modifier measurements, assuming a collector heat removal factor F_r of 0.99[19], a solar absorptance, α_1, of 0.8[4, 20] and a back reflector reflectance, ρ_4, of 0.8[21]. Predicted and experimental normal incidence results differ only be 2%. The agreement for the transversal transmittance is good except at θ equal to 50° where the model underpredicts the experiment by 8%.

These comparisons provide confidence in the ray tracing algorithm.

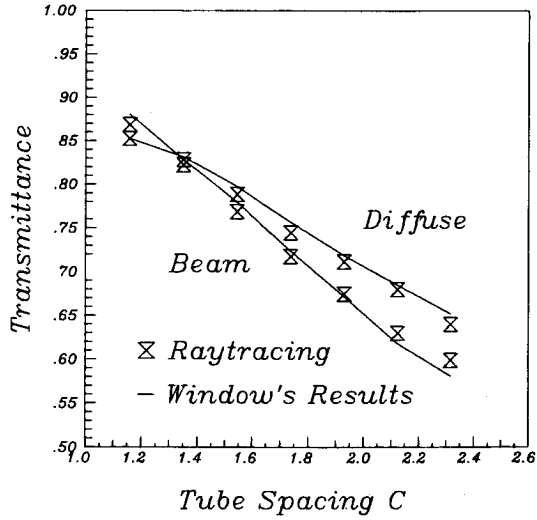

Fig. 7. Comparison between ray tracing and Window's [9] results for beam and diffuse transmittance of an ETC array with diffuse back reflector ($W = 0.77$, $\rho_4 = 0.8$).

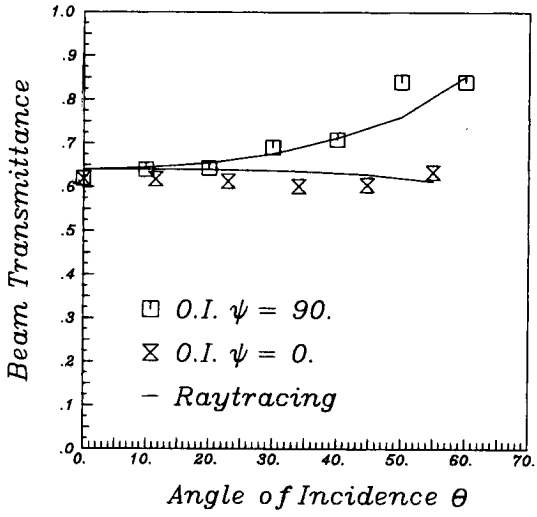

Fig. 8. Prediction of the transmittance properties of Owens-Illinois' Sunpack Model 1004 Series Collector [21] with the ray tracing model ($W = 0.81$, $C = 1.9$, $\rho_4 = 0.8$).

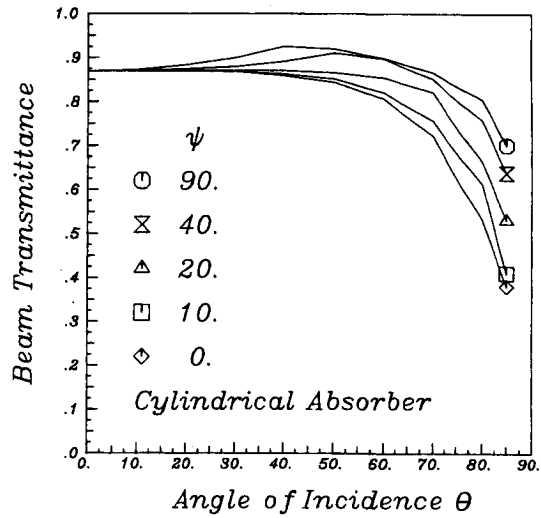

Fig. 10. Beam transmittance of an ETC array with cylindrical absorber ($W = 0.9$, $C = 1.2$, $\rho_4 = 0.8$).

V.2 *Beam transmittance*

The beam transmittance τ_1 of a flat absorbr ETC array, computed using Philips Heat Pipe ETC properties[6] (i.e. $C = 1$, $W = 0.9$, $\rho_4 = 0.8$) is presented in Fig. 9 versus θ and ψ. For θ less than 60°, τ_1 is almost independent of the azimuth angle and, hence, of the tube orientation. At values of θ greater than 60°, τ_1 is a function of ψ for ψ less than 40°.

Figure 10 presents the beam transmittance for the same array as in Fig. 9 with cylindrical absorbers. The curves are no longer independent of the azimuth angle. The transversal transmittance ($\psi = 90$) has a normal value of 0.870 and a maximum at about $\theta = 30°$. The reason for the normal beam transmittance for the cylindrical absorber being greater than that for the flat absorber is that the view factor between the back reflector and the absorber tubes is greater than the view factor between the back reflector and the flat absorber.

V.3 *Diffuse transmittance*

As was done for the tubular cover, the tube direction is assumed perpendicular to the intersection between the collector plane and the horizon. The sky diffuse, τ_2, and ground diffuse, τ_3, transmittances are given in Fig. 11 for a flat absorber and in Fig. 12 for a cylindrical absorber ETC array computed with the same parameters as used in Figs. 9 and 10. For both absorber shapes, the sky diffuse transmittance is independent of the collector slope. This is similar to the behavior of the flat plate collector and tubular cover. The higher transmittance of the cylindrical absorber when compared to the flat absorber is again due to the difference between their back reflector-to-absorber view factors. As

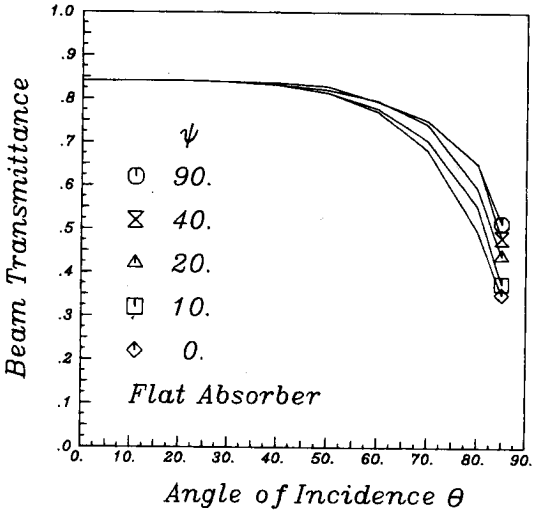

Fig. 9. Beam transmittance of an ETC array with flat absorber ($W = 0.9$, $C = 1.2$, $\rho_4 = 0.8$).

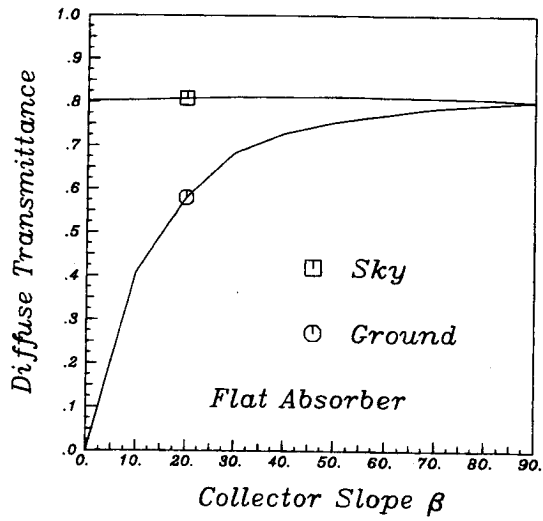

Fig. 11. Diffuse transmittance of an ETC array with flat absorber ($W = 0.9$, $C = 1.2$, $\rho_4 = 0.8$).

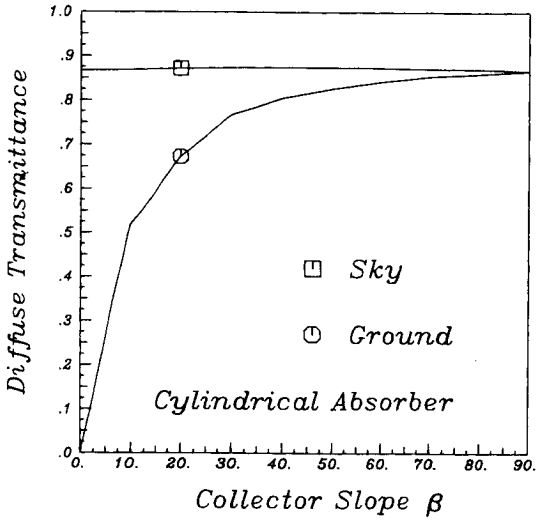

Fig. 12. Diffuse transmittance of an ETC array with cylindrical absorber ($W = 0.9$, $C = 1.2$, $\rho_4 = 0.8$).

will be shown in the next section, τ_2 is a function of the array geometry, mostly through the view factor from the back reflector to absorber, F_{41}, and the back reflector reflectance ρ_4. Increasing F_{41} (i.e. increasing W/C) and/or ρ_4 increases τ_2. The ground diffuse transmittance is approximately equal to the sky diffuse transmittance for slopes greater than 40°, and goes to zero at a slope of zero.

V.4 *analytical expressions for the partition matrix*

As shown by eqn (5) the four transmittances are functions of the back reflector reflectance ρ_4 and the partition matrix R, which is in turn related to sizing parameters of the array and the angular description of the light sources. This section discusses the functional form of the curve fits for each element of the partition matrix. The final curve fits for each matrix element are given in the appendix.

The glass absorption will be neglected in the following development with the consequence:

$$R_{i2} = 0, \qquad \text{for all } i. \tag{9}$$

The R_{1j} row of the matrix distributes the incoming beam radiation between the three remaining light sinks, the glass being neglected. The portion of the beam intercepted by the absorber is expressed as the product of four factors:

$$R_{11} = \tau_1'(\theta, \psi, W_p)X_a(\theta_t, W, C) \times X_r(\theta_x, C)X_s(\theta_t, W, C), \tag{10}$$

where τ_1' is the transmittance of a single tube (as was presented in Fig. 6). The transversal incidence angle, θ_t, is given by $\theta_t = \tan^{-1}(\tan\theta \sin\psi)$ and the axial incidence angle, θ_x, is given by $\theta_x \sin^{-1}(\sin\theta \cos\psi)$. The factor X_a takes into account the actual absorber area seen by the incoming radiation, X_r introduces the effect of external multiple reflections between the tubes of the array and X_s accounts for shading between adjacent tubes. Each of these factors was computed using ray tracing results, and each was curve fitted as a function of the indicated variables. The beam radiation that is reflected back to the surroundings, R_{13}, is a function of the geometry and the incidence angle only:

$$R_{13} = f(\theta, W, C). \tag{11}$$

The R_{14} element is computed using eqn (1).

The R_{2j} elements of the matrix distribute the sky diffuse radiation to the various sinks. Following the conclusions of section V.3, the R_{2j}'s are assumed independent of the slope and are only functions of the geometry. The sky diffuse radiation intercepted by the absorber is proportional to the view factor between the absorber and the surroundings, F_{13}, which is a function of the array geometry.

$$R_{21} = f(W/C). \tag{12}$$

The reflected diffuse radiation R_{23} is a linear function of the view factor F_{23} from the glass tubes to the surroundings, which is only a function of the tube spacing

$$R_{23} = f(C). \tag{13}$$

The sky diffuse light reaching the reflector, R_{24} is found using eqn (1).

The partition of ground diffuse radiation R_{3j} is obtained by multiplying the R_{2j} row by shape factors which are functions of the slope and the internal size of the array.

Finally, the R_{4j}'s, which distribute the reflected light from the back reflector, are obtained by eqn (7).

Comparisons between transmittances determined using the ray tracing algorithms and eqn (5) are presented in Figs. 13 and 14 for a wide variety of cylindrical absorber array designs and with $\rho_4 = 0.8$. The standard deviation, σ, between the ray tracing and predicted values is less than 1%. A similar result was found for the flat absorber. This low standard deviation indicates that the proposed model is suitable for design purposes.

V.5 *Beam transmittance interpolation algorithm*

Testing standards for optically asymmetric collectors result in longitudinal and transversal incidence angle modifiers. In order to obtain the transmittance at any incidence angle, it is necessary to have an angular interpolation algorithm. McIntire[10] concluded that for nonimaging concentrating collectors the product of the two incidence angle modifiers is a good approximation to the actual incidence angle modifier provided the proper

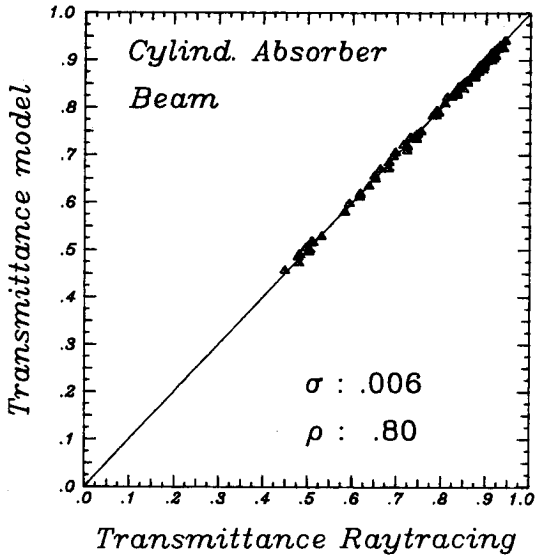

Fig. 13. Comparison of beam transmittances predicted with the R_{ij} model and ray tracing ($0.6 < W < 1$; $0.3 < W/C < 1$; $\rho_4 = 0.8$).

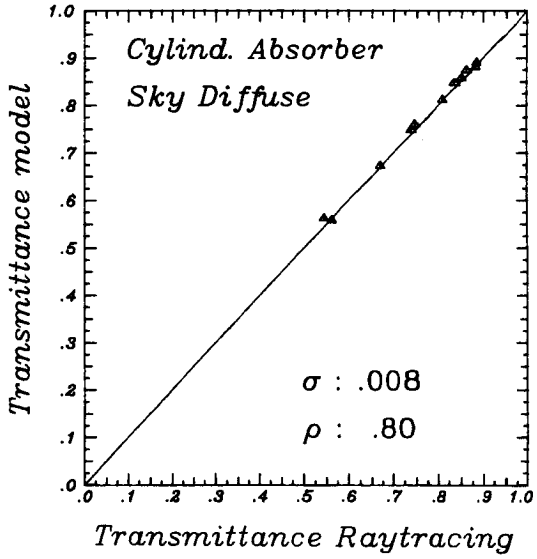

Fig. 14. Comparison of sky diffuse transmittances predicted with the R_{ij} model and ray tracing ($0.6 < W < 1$; $0.3 < W/C < 1$; $\rho_4 = 0.8$).

angular projections are used. Thus,

$$K_{\tau\alpha}(\theta, \psi) = K_{\tau\alpha}(\theta_l, 0°)K_{\tau\alpha}(\theta_t, 90°) = K_{\tau\alpha l}(\theta_l)K_{\tau\alpha t}(\theta_t), \quad (14)$$

where θ_l, the projection of the incidence angle θ in the longitudinal plane, is given by

$$\theta_l = \tan^{-1}(\tan\theta \cos\psi) \quad (15)$$

and θ_t, the projection of θ into the transversal plane, is given by§

$$\theta_t = \tan^{-1}(\tan\theta \sin\psi). \quad (16)$$

Comparisons between transmittances obtained by eqns (14), (15) and (16) and transmittances obtained by the ray tracing algorithm are shown in Fig. 15. The standard deviation is less than 1%.

V.6 *Effective beam direction for diffuse radiation*

In order to determine the diffuse transmittance from the incidence angle modifiers, an effective beam direction can be found so that the beam transmittance is equal to the diffuse transmittance. Figure 16 shows, in the $(\theta-\psi)$ plane, contours where the beam transmittance is equal to the sky diffuse transmittance. Each curve corresponds to a particular set of geometrical parameters with $\rho_4 = 0.8$. All of the lines intersect a small tringular area. Similar results were obtained for all values of the back reflector reflectance. Choosing $\theta = 60°$ and $\psi = 26°$ as the effective beam direction for diffuse radiation minimizes the standard deviation between the transmittance calculated by ray tracing and the transmittance obtained by choosing one particular direction. Equations (15) and (16) then give the effective beam directions as $\theta_l = 57°$ and $\theta_t = 37°$.

§ Equations (15) and (16) are in terms of a solar azimuth angle projected into the plane of the array. The orientation of this array plane is generally specified by the slope, β, and the azimuth, γ.

If the tubes are titled with a slope β in the array plane (i.e. if the tubes would intersect the ground if extended) then

$$\theta_l = |\beta - \tan^{-1}(\tan\theta_z \cos(\gamma - \gamma_s))|$$

$$\theta_t = \tan^{-1}\left(\frac{\sin\theta_z \sin(\gamma - \gamma_s)}{\cos\theta}\right)$$

where θ_z is the solar zenith angle and γ_s is the solar azimuth. Expressions for θ_z and γ_s are given in reference [14]. If the tubes are mounted horizontally on the array plane then θ_l becomes θ_t and θ_t becomes θ_l.

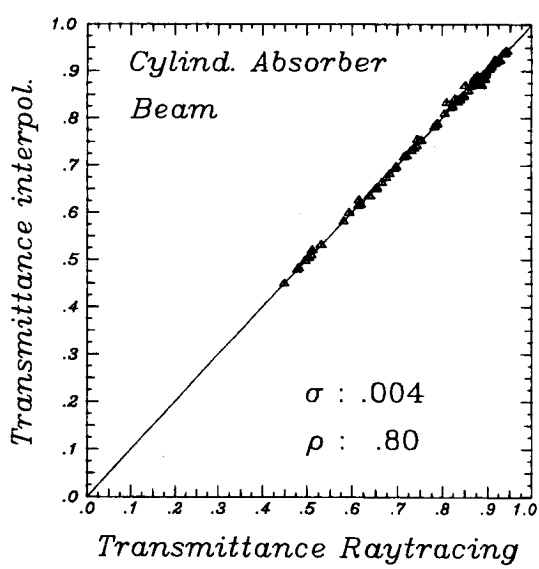

Fig. 15. Comparison of beam transmittances obtained by the biaxial product approximation and ray tracing ($0.6 < W < 1$; $0.3 < W/C < 1$; $\rho_4 = 0.8$).

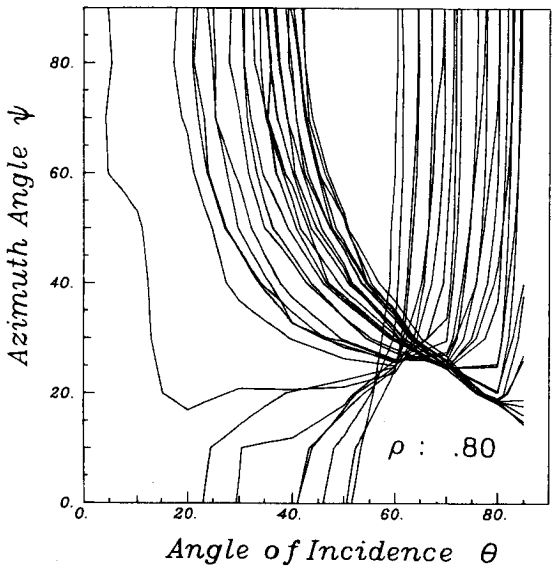

Fig. 16. Contours of equal beam transmittances and diffuse transmittances for different geometrical conditions ($0.6 < W < 1$; $0.3 < W/C < 1$; $\rho_4 = 0.8$).

Thus, starting from $K_{\tau\alpha t}$ and $K_{\tau\alpha l}$, the product approximation can be used for the effective beam direction to find the sky diffuse transmittance by

$$\tau_2 = \tau_1(0, 0)K_{\tau\alpha t}(37)K_{\tau\alpha l}(57). \quad (17)$$

Finally, the ground diffuse transmittance may be assumed equal to the sky diffuse transmittance. The error in this approximation is always less than 1% for a ground reflectance of 0.2.

VI. CONCLUSIONS

The partition matrix between light sources and sinks was introduced in order to analyze the transmittance features of optically asymmetric collectors. The computation of the matrix elements was performed by ray tracing. The algorithm was tested against previously published experimental and numerical results. Curve fits to the ray tracing results are presented that can be used to perform parametric studies.

The biaxial incidence angle modifier product, introduced by McIntire for specularly reflecting concentrator collectors, is extended to ETC arrays with a diffuse back reflector.

The effective beam direction for diffuse radiation was determned to be at an incidence angle of 60° with an azimuth angle 26°. These angles are equivalent to a transversal incidence angle of 37° and a longitudinal incidence angle of 57°. The diffuse transmittance of ETC arrays with diffuse back reflectors can be found from test results of the longitudinal and transversal incidence angle modifiers using the biaxial product approximation. The ground diffuse transmittance may be assumed equal to the sky diffuse transmittance without introducing significant errors.

NOMENCLATURE

- b_0 incidence angle modifier coefficient
- C dimensionless spacing between tube center lines
- D dimensionless distance between the tube center line and the back reflector
- F_{13} view factor between absorber and surroundings
- F_{23} view factor between glass tubes and surroundings
- $K_{\tau\alpha}$ incidence angle modifier
- $K_{\tau\alpha l}$ incidence angle modifier in the longitudinal plane
- $K_{\tau\alpha t}$ incidence angle modifier in the transversal plane
- R_{ij} partition matrix element between the light source i and light sink j
- W dimensionless width or diameter of the absorber
- W_p absorber width or diameter projected in the beam direction

Greek symbols

- α_i absorptance of the absorber
- β slope of the collector
- θ angle of incidence
- θ_l longitudinal incidence angle
- θ_t transversal incidence angle
- θ_x axial incidence angle
- ρ_4 diffuse back reflector reflectance
- ρ_g ground diffuse reflectance
- $\bar{\tau}$ beam transmittance of a tubular cover computed by splitting the radiation into its parallel and perpendicular components
- $\tau_\parallel$ transmittance of a tubular cover for the parallel component of the radiation
- $\tau_\perp$ transmittance of a tubular cover for the perpendicular component of the radiation
- τ_1' beam transmittance of a single ETC
- τ_1 beam transmittance
- τ_2 sky diffuse transmittance
- τ_3 ground diffuse transmittance
- ψ incidence azimuth angle in the collector plane between longitudinal plane and plane of collector normal and the beam radiation

REFERENCES

1. D. Godolphin, Rising hopes for vacuum tube collectors. *Solar Age* 31–35 (June 1982).
2. C. S. Herrick. Optical transmittance measurements on a solar collector cover of cylindrical glass tubes. *Solar Energy* **28**(1), 5–11 (1982).
3. D. Jones, in *Annual DoE Active Solar Heating and Cooling Contractor's Review Meeting*. pp. 9–53, NTIS CONF-800340 (26–28 March, 1980).
4. W. R. McIntire and K. Reed, Incidence angle modifiers for evacuated tube collectors. AS-ISES Annual Meeting, Philadelphia, PA pp. 282–284 (1981).
5. B. Window and I. M. Bassett, Optical collection efficiencies of tubular solar collectors with specular reflectors. *Solar Energy* **26**, 341–346 (1981).
6. J. C. De Grijs, H. Bloem and R. De Vann, Evacuated tubular collector with two-phase heat transfer into the system. *ISES World Forum*, Brighton, U.K. (1982).
7. Solar System for Building, Industry & Agriculture 81.03.B, Sanyo Electric Air Conditioning Equipment Co., Ltd., Division of Sanyo Electric Co., Ltd., 3-10-15 Hongo, Bunkyo-Ku, Tokyo, Japan 113.
8. F. Mahduri, Evacuated heat pipe solar collector. Solar Energy & Conservation Symposium—Workship, 11–13 December, 1978, Miami Beach, FL, U.S.A.
9. B. Window and J. Zybert, Optical collection efficien-

cies of arrays of tubular collectors with diffuse reflectors. *Solar Energy* **26,** 325–331 (1981).
10. W. R. McIntire, Factored approximations for biaxial incidence angle modifier. Personal communication (1983).
11. M. J. Brandemuehl and W. A. Beckman, Transmission of diffuse radiation through CPC and flat-plate collector glazings. *Solar Energy* **24,** 511–513 (1980).
12. Gebhart, B. *Heat Transfer*. 2nd ed., pp. 150–163, McGraw-Hill, New York (1971).
13. M. B. Eberlein, Analysis and Performance Predictions of Evacuated Tubular Collectors Using Air as the Working Fluid. M.S. Thesis, University of Wisconsin (1976).
14. J. A. Duffie and W. A. Beckman, *Solar Engineering of Thermal Processes*. Wiley, New York (1980).
15. W. A. Shurcliff, Transmittance and reflection loss of multi-plate planar window of a solar radiation collector: Formulas and tabulations of results for the case $n = 1.5$". *Solar Energy* **16,** 149–154 (1974).
16. P. H. Theunissen, Letter to the Editor, *Solar Energy*, **30,** 294 (1983).
17. F-Chart 4.1, A Design Program for Solar Heating Systems. Solar Energy Laboratory, University of Wisconsin-Madison (June 1982).
18. J. D. Felske, Analysis of an evacuated cylindrical solar collector. *Solar Energy* **22,** 567–570 (1979).
19. L. Spanoudis, Owens-Illinois, Personal Communication (June 1982).
20. B. Window and G. L. Harding, Materials Science Aspects in All Glass Evacuated Tube Collectors. School of Physics, University of Sidney, Preprint of Manuscript submitted to *Solar Energy* (1982).
21. A Glass Pipeline to the Sun, Sunpack Brochure 13.11a/OI, Owens-Illinois.

APPENDIX

Analytical expression of the partition matrix $R(\theta_x < 60, \theta_t < 60)$

1. *Flat absorber*†

$$R_{11} = \tau_t'(\theta, \psi, W)X_a(W, C)X_r(\theta_x, C)X_s(\theta_t, W, C)$$

$$\begin{aligned}\tau_t'(\theta, \psi, W) &= (0.922 - 0.040W_p^{11.5}) \\ &\quad \times [1 - (0.0798 + 0.0770W_p^{2.5}) \\ &\quad \times (1/\cos\theta_x - 1)] \\ &\quad + 0.0748\theta^{2.71}e^{3.08(W-1)} \\ &\quad \times (1 - \cos\theta_t)/\cos\theta_t\end{aligned}$$

$$W_p = W\cos\theta_t$$

$$X_a(W, C) = W/C$$

$$X_r(\theta_x, C) = 1 + 0.435e^{-2.37C}(1 + 1.92\theta_x^{1.94})$$

$$\begin{aligned}X_s(\theta_t, W, C) &= 1 - \max[0, 0.42 \\ &\quad - ((0.77C - 0.353W)\cos\theta_t)]\end{aligned}$$

$$R_{12} = 0$$

$$R_{13} = (1 + 1.140^2)(1 + 0.144e^{-CW})(0.056/C)$$

$$R_{14} = 1 - R_{11} - R_{13}$$

$$R_{21} = 0.908F_{12}$$

$$F_{12} = W/C$$

$$R_{22} = 0$$

$$R_{23} = 0.140F_{23} - 0.025$$

$$F_{23} = [\pi/2 - \sin^{-1}(1/C) + (C^2 - 1)^{1/2} - C]/C$$

$$R_{24} = 1 - R_{21} - R_{23}$$

$$R_{31} = R_{21}(1 - \max[1 - (C - 1)/1.52, 0]e^{-\beta/0.305})$$

$$R_{32} = 0$$

$$R_{33} = R_{23}(0.332\,\beta + 1.05)/\beta$$

$$R_{34} = 1 - R_{31} - R_{33}$$

$$R_{41} = R_{21}$$

$$R_{42} = 0$$

$$R_{43} = R_{24}$$

$$R_{44} = 1 - R_{41} - R_{43}$$

† The meaning of the function max $[x, y]$ is that x should be used if $x \geq y$ and y should be used if $y > x$.

2. *Cylindrical absorber*

$$R_{11} = \tau_t(\theta, \psi, W)X_a(\theta_t, W, C)X_r(\theta_x, C)X_s(\theta_t, W, C)$$

$$\begin{aligned}\tau_t'(\theta, \psi, W) &= (0.922 - 0.040W^{11.5}) \\ &\quad \times [1 - (0.0798 + 0.0770W^{2.5}) \\ &\quad \times (1/\cos\theta_x - 1)]\end{aligned}$$

$$X_a(\theta_t, W, C) = \min[1, W/(C\cos\theta_t)]$$

$$X_r(\theta_x, C) = 1.01 + 0.539e^{-2.41C}(1 + 2.28\theta_x^2)$$

$$\begin{aligned}X_s(\theta_t, W, C) &= 1 \text{ if } X_i < 0 \\ &= [0.411(W - X_i)/(X_aC\cos\theta_t) \\ &\quad + 0.589](1 - 0.056X_i)\end{aligned}$$

$$X_i = (W + 1)/2 - C\cos\theta_t$$

$$R_{12} = 0$$

$$R_{13} = 0.056\,(1 + 0.8960^2)(1 + 0.061e^{-CW})/C$$

$$R_{14} = 1. - R_{11} - R_{13}$$

$$R_{21} = 0.890F_{12}$$

$$F_{12} = W/C[\pi/2 - \sin^{-1}(W/C) + ((C/W)^2 - 1)^{1/2} - C/W)]$$

$$R_{22} = 0$$

$$R_{23} = 0.118F_{23} - 0.018$$

$$F_{23} = [\pi/2 - \sin^{-1}(1/C) + (C^2 - 1)^{1/2} - C]/C$$

$$R_{24} = 1 - R_{21} - R_{23}$$

$$R_{31} = R_{21}[1 - (1 - (C - 1)/0.73 - (1 - W)/0.51)]e^{-\beta/0.297}$$

$$R_{33} = R_{23}(0.332\beta + 1.05)/\beta$$

$$R_{34} = 1 - R_{31} - R_{33}$$

$$R_{41} = R_{21}$$

$$R_{42} = 0$$

$$R_{43} = R_{24}$$

$$R_{44} = 1 - R_{41} - R_{43}$$